

1 **Field and genetic evidence support the photosynthetic performance index**
2 **(PI_{ABS}) as an indicator of rice grain yield**

3

4 Rodríguez, Andrés Alberto^{1*}; Vilas, Juan Manuel¹, Sartore, Gustavo Daniel², Bezus,
5 Rodolfo², Colazo, José³, Maiale Santiago Javier¹

6

7 ¹ Laboratorio de Fisiología y Asistencia al Mejoramiento Vegetal, Instituto
8 Tecnológico de Chascomús (CONICET-UNSAM), Escuela de Bio y Nanotecnologías
9 (UNSAM)

10 ² Facultad de Ciencias Agrarias y Forestales, Universidad Nacional de la Plata, 60 y
11 119, La Plata, Pcia. Bs. As., Argentina

12 ³ EEA INTA Concepción del Uruguay, Ruta 39 Km 143, Concepción del Uruguay,
13 Pcia. de Entre Ríos, Argentina

14

15

16 * **Corresponding author:**

17 Dr. Andrés Alberto Rodríguez

18 Laboratorio de Fisiología y Asistencia al Mejoramiento Vegetal, INTECH-CONICET-
19 UNSAM; Escuela de Bio y Nanotecnologías (UNSAM), Intendente Marino Km 8.2-
20 B7130IWA, Chascomús, Argentina; Tel: +54 2241 430323; Fax: +54 2241 424048.
21 Email: andresrodriguez@conicet.gov.ar

22

23 **ABSTRACT**

24 The effective increase of the rice breeding process for grain yield could be sustained
25 by developing efficient tools to accelerate plant selection through the rapid
26 determination of reliable predictors. Here, we have described different associations
27 between grain yield and photosynthetic parameters simply and fast obtainable by a
28 non-invasive technique in flag leaf during the anthesis stage. Among the analyzed
29 photosynthetic parameters, the photosynthetic performance index (PI_{ABS}) stood out
30 for its strong association with grain yield. A genome-wide association analysis
31 determined in plants from a rice diversity panel at tillering stage indicated the
32 presence of a quantitative trait locus on chromosome 9 characterized by a set of

33 candidate chloroplastic genes with contrasting haplotypes for PI_{ABS} . An analysis of
34 these haplotypes indicated a separation into two groups. One with haplotypes linked
35 to high values of PI_{ABS} , which were associated almost exclusively with *Japonica* spp.
36 subpopulations, and another with haplotypes linked to low values of PI_{ABS} , which
37 were associated exclusively with *Indica* spp. subpopulations. Genotypes of the
38 *Japonica* spp. subpopulations showed high values in panicle weight, a yield
39 components parameter, compared with the *Indica* spp. subpopulations genotypes.
40 The results of this work suggested that PI_{ABS} could be an early predictor of grain yield
41 at the tillering stage in rice breeding processes.

42

43 **Keywords:** *Oryza sativa*, sustainable crops, photosynthetic performance index
44 (PI_{ABS}), grain yield predictors.

45

46

47 **Abbreviations:** GWAS, genome-wide association analysis; LD, linkage
48 disequilibrium; MAF, minor allele frequency; PW, panicle weight; PI_{ABS} ,
49 photosynthetic performance index; PCA, principal component analyses; QTL,
50 quantitative trait locus; RC, active PSII reaction centre; RDP1, Rice Diversity Panel
51 1; SNPs, single nucleotide polymorphism; WFG, weight of filled grains; Y, Kg of
52 grains per ha⁻¹.

53

54

55

56

57 **1. Introduction**

58 Current evidence shows that there is a genetic background in the main cultivated
59 species to improve the sustainability of their crops by increasing their yields through
60 an improvement in the environmental adaptation of plants to the environments in
61 which they are grown. However, the screening for higher yields under field conditions
62 often imposes troubles due to the variability of climate, edaphic conditions and
63 management practices (Tavakkoli et al., 2012). In the case of the rice species *Oryza*
64 *sativa*, there is also the fact that its genotypes differ enormously in the levels of grain
65 yield owing to the vast diversity of genetic constitutions (Xing and Zhang, 2010). The
66 use of indirect selection criteria in breeding for better yields was reported in rice

67 (Shen et al., 2001). However, for indirect selection to be successful, the specific traits
68 must have a high correlation with yield (Richards et al., 2001). Therefore, developing
69 robust physiological indicators of easy and rapid determination that correlate with
70 yield parameters in the field could be a practical indirect approach for mass
71 screening populations as significant as used in breeding programs.

72 Field experiments have shown that high yield in rice is causally related to the
73 protection of the photosynthetic apparatus through excess light dissipation (Wang et
74 al., 2014). The OJIP test is a technique that depicts different OJIP parameters linked
75 with the state of structures and functionalities related to the photosystem II (PSII)
76 complex (Calzadilla et al., 2022). It includes functional parameters such as F_V/F_M and
77 ΨE_0 and structural parameter as γRC . F_V/F_M represents the maximum photochemical
78 efficiency of PSII, which represents the maximum efficiency with which an absorbed
79 photon result in the reduction of the quinone A. ΨE_0 represents the maximum
80 efficiency of electron transport in PSII beyond reduced quinone A, and γRC reflects
81 alterations in the density of active PSII reaction centre (RC) through changes in the
82 active chlorophyll associated to the RC (Strasser et al., 2000). Besides, Živčák et al.
83 (2008) reported the photosynthetic performance index (PI_{ABS}) derived from the union
84 of γRC , F_V/F_M and ΨE_0 in a single equation $PI_{ABS} = (\gamma RC / 1 - \gamma RC) \cdot (F_V/F_M / 1 -$
85 $F_V/F_M) \cdot (\Psi E_0 / 1 - \Psi E_0)$. These authors described the PI_{ABS} as an integrative and
86 sensitive parameter to register the combined changes of these last three OJIP
87 parameters in a unique value of plant vitality. Some authors have shown that super-
88 high-yielding hybrid rice flag leaves are causally related to PI_{ABS} (Zhang et al., 2015).
89 Parent's election in breeding programs depends on screening and selecting
90 genotypes with better performance characteristics. However, for selective breeding
91 to be practical, genetic variation must be present in the screened population (Hill,
92 2001). In the case of *O. sativa*, the genetic diversity is encompassed by two
93 subspecies and five subpopulations. The subspecies *Japonica ssp.* groups include
94 the subpopulations temperate Japonica, aromatic and tropical Japonica and the
95 subspecies *Indica ssp.* groups include the subpopulations indica and aus (Garris et
96 al., 2005). These five subpopulations are well represented in the rice diversity
97 germplasm collection called Rice Diversity Panel 1 (RDP1), which contains 413
98 genotypes. The RDP1 spans a wide genetic variability based on the diversity of
99 environmental growth conditions at the origin and breeding histories of *O. sativa*
100 accessions (Zhao et al., 2011).

101 In order to evaluate potential physiological parameters as indirect yield indicators
102 with easy and rapid determination related to structural and functional parameters
103 linked to PSII, we performed two experiments (Experiments 1 and 2). Experiment 1
104 was performed to characterize the relationship between yield parameters with
105 structures and functionalities of the PSII determined at anthesis in the flag leaf of rice
106 genotypes with contrasting grain yield in the field plot. In Experiment 2, different
107 genome-wide association analysis (GWAS) was performed using a phenotypification
108 determined at the tillering stage in a leaf of plants from RDP1 genotypes based on
109 photosynthetic parameters, particularly PI_{ABS} . This last experiment was designed to
110 generate meaningful information about the connections of the rice population
111 structure with the relationship between yield and the PSII performance and with the
112 PI_{ABS} capacity as an early predictor of grain yield during the tillering stage in rice
113 breeding processes.

114

115

116 **2. Materials and Methods**

117

118 **2.1. Plant material and growth conditions**

119 Seeds of 10 rice genotypes with contrasting grain yields were used in Experiment 1.
120 The selected genotypes were H458, H426-1-1-1, Don Ignacio, H294, R-03, Don
121 Justo, H426-25, Yerua and H420. The selected genotypes were the cultivars Don
122 Ignacio FCAYF, Don Justo FCAYF and Yerúa and the inbreed lines H458, H426-1-1,
123 H294, H426-25, R-03 and H420, all belonging to FCAYF rice breeding program.
124 Seeds from all genotypes were mechanically sown in plots of 20 square meters in a
125 randomized design with three replications with 20 cm in the space between rows and
126 with a density of 300 seeds m^{-2} . The amounts of fertilizer applied as a basal dressing
127 were 6.84 g N m^{-2} , 2.7 g P m^{-2} and 8.5 g K m^{-2} . The trial was conducted under
128 flooding until the maturity stage.

129 Seeds of 283 genotypes were used in Experiment 2, these comprising 45 aus, 59
130 indica, 58 temperate and 76 tropical japonica, eight aromatic and 37 admixed rice
131 genotypes. Seeds from all genotypes were sown in Petri dishes on two layers of
132 Whatman N° 5 filter paper, rinsed with 7 mL carbendazim 0.025 %p/v and incubated
133 at 30 °C in darkness for three days until germination. Each resultant seedling was
134 transplanted into a plastic pot (10 L) containing sterilized organic soil extract as

135 substrate. The pots were transferred to field environmental conditions into a plot in a
136 completely randomized design with three replications, and the trial was conducted
137 under flooding until the maturity stage.

138

139 **2.2. Determination of photosynthetic parameters**

140 The photosynthetic parameters were determined by analyzing the chlorophyll
141 fluorescence emission kinetics according to Gazquez et al. (2015). A portable
142 fluorometer was used, HANDY PEA (Hansatech Instruments® Ltd., King's Lynn,
143 Norfolk, UK). Briefly, blade sections of intact leaves were covered with a leaf clip to
144 adapt them to darkness for 20 min. The flag leaf represented the intact leaves at the
145 anthesis stage (Experiment 1) or the uppermost fully expanded leaf in 11-week-old
146 plants at tillering stage (Experiment 2). Then, the blade sections were exposed to a 3
147 s pulse of red light (650 nm, 3500 $\mu\text{mol photons m}^{-2} \text{s}^{-1}$). The raw fluorescence data
148 of the fluorescence emission kinetic was processed by the PEA plus software
149 (Hansatech Instrument, UK) to determine the different OJIP parameters. The OJIP
150 parameters described above, γRC , F_v/F_M and ΨE_0 , were calculated according to the
151 equations described by Puig et al. (2021).

152

153 **2.3. Determination of yield parameters**

154 In all experiments, plants were harvested, panicles were threshed manually, and the
155 grain was dried in an oven at 40 °C until 14% humidity. For Experiment 1, the yield
156 parameters were determined per plot as the number of grains per square meter
157 ($\text{Grains} \cdot \text{m}^{-2}$) and the Kg of grains per ha^{-1} (Y). For Experiment 2, the number of
158 panicles (NP) and the weight of filled grains (WFG) were determined per plant at
159 harvest. Then, the panicle weight (PW) was calculated as $\text{PW} = \text{WFG} \cdot \text{NP}^{-1}$.

160

161 **2.4. Genome-wide association and linkage disequilibrium analyses**

162 The GWAS studies and the linkage disequilibrium (LD) were performed based on the
163 HDRA dataset (HDRA6.4) genotyping from the RDP1 genotypes consisting of
164 700,000 single nucleotide polymorphism (SNPs) described by McCouch et al. (2016).
165 Three replicates of the complete set of samples were used to perform the
166 phenotyping data for each trait. GWAS mapping was performed considering settings

167 and recommendations described by McCouch et al. (2016) using the Tassel software
168 (Tassel v5.0). Briefly, GWAS was running using a linear mixed model in the EMMAX
169 algorithm (Kang et al., 2010), which considers the underlying population structure by
170 including a kinship matrix as a covariate. A minor allele frequency (MAF) threshold of
171 0.05 ($MAF < 0.05$) was applied to discard markers with exceedingly rare alleles.
172 When the GWAS were run across all available RDP1 genotypes, SNPs at $MAF >$
173 0.05 in individual subpopulations were combined. Then, three additional principal
174 component covariates, derived from a principal component analysis (PCA) to
175 characterize the RDP1 genetic structure, were added to the model. Based on the
176 approximate significance value where the observed p-values exceed the expected
177 number in the Q-Q plots, a significance threshold of 10^{-4} was used to identify
178 significant SNP across all analyses. The quantitative trait locus (QTL) determined in
179 the GWAS peak on chromosome 9 were delimited according to McCouch et al.
180 (2016). Regions with significant SNPs were identified as having three or more
181 significant SNPs in a 200 kb region. They overlapped when they shared significant
182 SNPs to form a single QTL region. GWAS LD among markers on chromosome 9 was
183 calculated using pairwise r square between SNPs and the LD analysis function with
184 an LD windows size of 500 SNPs in the Tassel software.

185

186 **2.5. Gene targeting, gene annotation and haplotype analyses**

187 The genes within the QTL regions were identified using the data of the RICEBASE
188 (www.ricebase.org) database and a protein subcellular localization prediction
189 analysis. The protein sequence of each gene was downloaded from the MSU Rice
190 Genome Annotation Project version 7. The protein subcellular localization prediction
191 analysis was performed, integrating all information of these protein sequences from
192 the databases: WoLF PSORT, Plant-mPLOC and TargetP. Gene annotation about the
193 GWAS peak genes was performed, integrating all information from the databases:
194 Gramene, Uniprot and KEEG. Haplotypes from all genes with the predicted
195 chloroplastic location were collected and entered along with their associated PI_{ABS}
196 average values into statistical analysis software to select genes with contrasting
197 haplotypes in PI_{ABS} .

198

199 **2.6. Statistics**

200 All data sets were tested for normality. Data from photosynthetic and yield
201 parameters, including the PI_{ABS} average values associated with haplotypes of genes
202 with contrasting haplotypes in PI_{ABS} , were subjected to ANOVA and post hoc
203 analyses DGC tests (Di Rienzo, Guzmán, Casanoves, 2002) and to Student's t-test.
204 These data were also subjected to linear correlation analyses, principal component
205 analyses (PCA), and some linear regression analyses using the Infostat® statistical
206 software package used throughout the study (Di Rienzo et al., 2018).

207

208

209 **3. Results**

210

211 **3.1. Experiment 1. Relationship between the yield with structures and** 212 **functionalities of the photosystem II in the flag leaf of contrasting rice** 213 **genotypes in grain yield**

214 A PCA showed that the variability associated with the set of all parameters separated
215 the data of genotypes with above-average yield or high yield (HY, 10 Tn/ha on
216 average) from genotypes with below-average yield or typical yield (NY, 8.3 Tn/ha in
217 average). The data separation was due to PC1, which retained 71.3% of the total
218 dataset variability (Fig. 1). The reported eigenvectors associated with each original
219 variable weighted to form PC1 indicated PI_{ABS} , Ψ_{E_O} , F_V/F_M , γ_{RC} and Kg of grains .
220 m^{-2} (Y) received the highest weights (Table S1). On the other hand, Y explained
221 18.5% of the variability retained by PC2. Therefore, these results suggested that
222 multiple parameters related to the PSII and mainly Y explained the distinction
223 between HY and NY genotypes mainly by the variability explained by PC1.

224 In addition, the PCA results revealed multiple associations between yield and PSII
225 parameters. Linear correlation analysis indicated many significantly positive
226 correlations among structure and functional parameters of the PSII in flag leaf with
227 yield parameters (Table 1). The most relevant results were the high correlations
228 between the Y with all PSII parameters, particularly with PI_{ABS} and Ψ_{E_O} ($r = 0.85$ in
229 both cases). This data was in line with another statistical analysis in which a
230 complementary model from different linear regression analyses indicated that 72% of
231 the variation of Y was explained by PI_{ABS} (Fig. 2). All these statistical results

232 suggested a relationship between yield and PSII parameters in which PI_{ABS} explained
233 most of the contrast observed.

234

235 **3.2. Experiment 2. Genome-wide association analysis using an OJIP** 236 **phenotypification in plants of RDP1 genotypes**

237 A GWAS performed using a phenotypification by PI_{ABS} determination in plants of
238 genotypes from the RDP1 rice diversity panel indicated the presence of multiple
239 significant molecular markers grouped in a GWAS peak on chromosome 9 that
240 involved 170 genes (Fig. 3A). Other complementary GWAS performed using
241 phenotypifications by ΨE_O , and γRC determinations also indicated multiple
242 significant molecular markers in common with PI_{ABS} in this GWAS peak on
243 chromosome 9 (Fig. 3A). A posterior analysis showed that 59 of these genes had a
244 predicted location in the chloroplast (Fig. 3B) and were in regions with high LD
245 values (Fig. 3C). Twenty per cent of genes found in this work could not be
246 characterized, and the remaining 80% were proteins related to functions in the
247 chloroplastid (Table 2). In addition, there were twenty chloroplastic genes with
248 contrasting haplotypes in PI_{ABS} ($CGPI_{ABS}$, Fig. 3D).

249

250 **3.3. Relationship between the haplotypes from the $CGPI_{ABS}$, panicle weight and** 251 **the rice population structure.**

252 The phenotypification in PI_{ABS} used in Experiment 2 was performed in RPD1 plants at
253 tillering stage that posteriorly was used to determine the yield component parameters
254 (YCP) panicle weight (PW) at the end of the grain filling stage. On the other hand,
255 this has allowed the characterization of the haplotype distribution derived from the
256 $CGPI_{ABS}$ within the rice population structure. On the other hand, it has also allowed
257 the characterization of the PW data distribution within the *O. sativa* subspecies and
258 subpopulations and then to compare these with the haplotype distribution.

259 A PCA was performed using two sets of PI_{ABS} data: the PI_{ABS} average high (HP) and
260 low (LP) values of each haplotype according to Fig. 3C and the particular PI_{ABS} of
261 each genotype. This analysis indicated that the variability associated with all
262 parameters agglomerated the data from HP and LP haplotypes in practically two
263 isolated groups. This phenomenon is because the LP haplotypes only presented a
264 few HP haplotype data, but the HP haplotypes did not group LP haplotype data (Fig.
265 4A). Another PCA was also performed using the previous two sets of PI_{ABS} data but

266 identifying genotypes of the five *O. sativa* subpopulations. This PCA indicated that
267 the group of HP haplotypes data were mainly composed of *Japonica* ssp. genotypes
268 from the temperate-japonica, tropical-japonica and aromatic subpopulations (Fig.
269 4B).

270 On the other hand, the group of LP haplotypes data was mainly composed of *Indica*
271 ssp. genotypes from indica and aus subpopulations. Data could suggest that HP and
272 LP haplotypes were related to *Japonica* spp. and *Indica* spp. subpopulations,
273 respectively. However, these results also suggested a relationship between HP and
274 LP haplotypes with PW because *Japonica* ssp. subpopulations presented higher PW
275 values than *Indica* ssp. subpopulations (Fig. 5).

276

277

278 **4. Discussion**

279 In the present work, we followed an approach based on different reports suggesting
280 that plant screening by chlorophyll fluorescence analysis in flag leaf could be
281 beneficial for breeding programs to improve grain productivity. The authors of these
282 reports indicated that the OJIP parameter PI_{ABS} could be a robust indirect indicator of
283 yield in rice (Zhang et al., 2015) but also in other crops such as wheat (Vuletić et al.,
284 2019) and oat (Tobiasz-Salach et al., 2019). Our work supported these results
285 suggesting that OJIP parameters determined in flag leaf, particularly PI_{ABS} , are
286 associated with grain yield parameters in rice. We have come to this conclusion after
287 examining the statistic PCA, linear correlation analysis and linear regression analysis
288 results that indicated a high positive correlation between all OJIP parameters,
289 particularly with Y. However, PI_{ABS} explained a significant part of Y variation
290 compared with the others OJIP parameters indicating that it could be the better
291 indirect indicator of yield in rice. This data also suggested that the relationship
292 between the photosynthetic activity and the grain yield would be explained by more
293 than one particular structure or functionality of PSII, particularly those represented by
294 PI_{ABS} .

295 The PI_{ABS} has been analyzed as a phenotypic trait through GWAS techniques in
296 different plant species studies (Liu et al., 2017; Chen et al., 2020; Zou et al., 2022)
297 but it is only recently that some authors have published works in rice (Vilas et al.,
298 2020; Khan et al., 2021). These last works indicated significant SNPs associated with
299 PI_{ABS} and other OJIP parameters and that many SNPs, including those linked to

300 PI_{ABS} , were associated with genes related to the chloroplast. Notably, Vilas et al.
301 (2020) indicated that some of these genes were $CGPI_{ABS}$. Khan et al. (2021) also
302 analyzed the PI_{ABS} distribution among *O. sativa* subpopulations indicating that the
303 *Japonica* spp. subpopulations had higher PI_{ABS} values than *Indica* spp.
304 subpopulations. However, needed to analyze the distribution of the HP and LP
305 haplotypes and yield parameters among these subpopulations. Our analyses
306 supported this result in terms of PI_{ABS} but, at the same time, suggested that this PI_{ABS}
307 distribution was linked to the HP and LP genotypes distributions because these were
308 associated mainly with the *Japonica* spp. and *Indica* spp. subpopulations,
309 respectively. Even more, because our data indicated that the *Japonica* spp.
310 subpopulations presented higher PW values than the *Indica* spp. subpopulations, this
311 led us to think that some $CGPI_{ABS}$ would explain the relationship between PI_{ABS} with
312 the yield parameters. However, even more interesting, all this suggested that PI_{ABS}
313 could be an early predictor of grain yield at the tillering stage in rice breeding
314 processes.

315 74% of our characterized $CGPI_{ABS}$ were annotated as a characterized protein. These
316 protein characterizations were analyzed using hypothetical processes that can
317 improve grain yield. Several $CGPI_{ABS}$ were characterized as small auxin-up RNA
318 (SAUR) proteins. The SAUR is a family of early auxin-responsive genes where
319 almost 70% of its members were subcellular and located in chloroplast, including the
320 SAURs in rice (*OsSAURs*) described by us (Zhang et al., 2021). Many SAUR
321 proteins were associated with developmental processes in rice, particularly in
322 reproductive development (Fujita et al., 2010; Courdet et al., 2011). The gene
323 LOC_Os09g37690 encodes a flavin-containing monooxygenase (FMO) similar to
324 FMO1 from Arabidopsis. The genes LOC_Os09g39230 and LOC_Os09g39260
325 encode arogenate dehydratase 5 (ADT5) from Arabidopsis. These last three genes
326 were also related to the *OsSAURs* described above because they play an essential
327 role in auxin biosynthesis (Zhao et al., 2001; Aoi et al., 2020). Some authors reported
328 that the content of endogenous auxin in rice plants during the early maturing period
329 is high (Dong et al., 2012), while other authors reported a PW increase in rice plants
330 sprayed with auxin (Ahmadi and Nejad, 2014). Therefore, all this information led us
331 to think that the set of $CGPI_{ABS}$ related to auxin biosynthesis could influence the
332 auxin level during panicle development. Consequently, they could influence the
333 panicle weight, as was determined in Experiment 2.

334 Another considerable number of CGPI_{ABS} were related to the functional and
335 structural quality of the chloroplast. Among these genes is found LOC_Os09g39570,
336 which encodes a β -amylase involved in starch hydrolysis and some authors related it
337 with panicle development in rice (Wang et al., 2019). Another three cases are the
338 genes LOC_Os09g38320, LOC_Os09g39670 and LOC_Os09g38330, which encode
339 a phytoene synthase, a short-chain dehydrogenase Tic32 and a protein
340 ACCUMULATION AND REPLICATION OF CHLOROPLASTS 3 (ARC3),
341 respectively. In the first case, the phytoene synthase is involved in the terpene
342 synthesis necessary for chloroplast differentiation (Chaudhary et al., 2019). A gene
343 encoding phytoene synthase was proposed in breeding strategies for improving rice
344 yield using agrobacterium-mediated transformation (Khan et al., 2015). Tic32 and
345 ARC3 are necessary at the chloroplast level because the first is an essential
346 Component in Chloroplast Biogenesis (Hörmann et al., 2004), and the second was
347 reported for its role in chloroplast division and expansion in *Arabidopsis* (Pyke and
348 Leech, 1994). Also, genes LOC_Os09g38540, LOC_Os09g39940 and
349 LOC_Os09g38980 encode proteins related to the biosynthesis of the component
350 from the photosynthesis process. The first two genes encode plastocyanin, an
351 electron transfer agent between cytochrome f of the cytochrome b6f complex from
352 PSII and P700⁺ from PSI. The third gene encodes a chloroplastic-like chaperonin,
353 which is an essential part of the system for folding the large subunit of ribulose 1,5-
354 bisphosphate (Zhao and Liu, 2017). Several reports indicate that the flag leaf's
355 photosynthesis constitutes 60 to 100% of the carbonated structures allocated in rice
356 grains (Wada et al., 1993; Takai et al., 2005). All these CGPI_{ABS} could influence the
357 photosynthetic apparatus performance, which could consequently act indirectly on
358 yield parameters.

359 A common feature of almost all CGPI_{ABS} described in this work was that they were
360 reported as candidate genes in different studies related to rice yield breeding in
361 different situations. For example, the gene LOC_Os09g37610 was recently identified
362 in rice breeding for grain-balanced elemental concentrations (Dwiningsih and
363 Alkahtani, 2022). The genes LOC_Os09g39070 and LOC_Os09g39240 were linked
364 with iron uptake in roots (Weirich et al., 2019). Many others as LOC_Os09g38420,
365 LOC_Os09g38510, LOC_Os09g39070, LOC_Os09g39180, LOC_Os09g39620,
366 LOC_Os09g39670, and LOC_Os09g39760, were reported in breeding studies to
367 improve rice for different abiotic and biotic tolerance (Wang et al., 2014; Du et al.,

368 2015; Raorane et al., 2015; Lakra et al., 2018; Gongora, 2015; Cal et al., 2019). Our
369 results suggested that all these genes could be candidates for use as molecular
370 markers in a molecular assistance process for rice breeding for grain productivity in
371 standard field conditions. In this regard, only the candidate gene LOC_Os09g39240
372 has been reported by a few authors for its relationship with rice breeding for grain
373 productivity under this condition (Ramos et al., 2019).

374

375

376 **5. Conclusions**

377 The challenge of improving rice plants for grain productivity involves developing
378 efficient tools that accelerate the plant selection process through the rapid
379 determination of robust indicators that allow the analysis of a large number of plants.
380 If such determinations involve a low cost per data point, the plant selection process
381 would have the potential to make scalable any breeding program. Here we have
382 found associations between grain yield and OJIP parameters determined in the flag
383 leaf, among which the PI_{ABS} stands out for its strong association with the yield. Early
384 phenotyping by determining PI_{ABS} in plants from a rice diversity panel led to the
385 characterization of a QTL with a set of various candidate chloroplastic genes with
386 contrasting haplotypes for PI_{ABS} . Combined analysis of these haplotypes in terms of
387 population structure in rice indicated that these were distributed within the
388 subpopulations of *O. sativa* similarly to the population structures described to PW.
389 This data suggested that the PI_{ABS} determination could be an early predictor of yield
390 in rice breeding processes. At the same time, the haplotypes of the candidate genes
391 associated with PI_{ABS} could also be used to perform molecular assistance in this
392 process. However, further studies are necessary to determine their effectiveness.

393

394

395 **6. Acknowledgements**

396 This work was financially supported by projects PICT 2019-02779, funded by
397 Agencia Nacional de Promoción Científica y Tecnológica, Argentina and PIP0363,
398 funded by Comision Nacional de Investigaciones Científicas y Técnicas.

399

400

401 **7. References**

- 402 [dataset] Ahmadi, N., Nejad, T.S., 2014. The effect of time and auxin spray on rice
403 yield factors in Iran. *Adv Environ Biol.* 457-461.
- 404 [dataset] Cal, A.J., Sanciangco, M., Rebolledo, M.C., Luquet, D., Torres, R.O.,
405 McNally, K.L., Henry, A., 2019. Leaf morphology, rather than plant water status,
406 underlies genetic variation of rice leaf rolling under drought. *Plant Cell Environ.* 42(5),
407 1532-1544.
- 408 [dataset] Calzadilla, P.I., Carvalho, F.E.L., Gomez, R., Neto, M.L., Signorelli, S.,
409 2022. Assessing photosynthesis in plant systems: a cornerstone to aid in the
410 selection of resistant and productive crops. *Environ Exp Bot.* 104950.
- 411 [dataset] Chaudhary, N., Nijhawan, A., Khurana, J.P., Khurana, P., 2010. Carotenoid
412 biosynthesis genes in rice: structural analysis, genome-wide expression profiling and
413 phylogenetic analysis. *Mol Genet Genomics.* 283(1), 13-33.
414 <https://doi.org/10.1007/s00438-009-0495-x>.
- 415 [dataset] Chen, S., Cheng, X., Yu, K., Chang, X., Bi, H., Xu, H., Wang, J., Pei, X.,
416 Zhang, Z., Zhan, K., 2020. Genome-wide association study of differences in 14
417 agronomic traits under low-and high-density planting models based on the 660k SNP
418 array for common wheat. *Plant Breed.* 139(2), 272-283.
419 <https://doi.org/10.1111/pbr.12774>.
- 420 [dataset] Coudert, Y., Bès, M., Van Anh Le, T., Pré, M., Guiderdoni, E., Gantet, P.,
421 2011. Transcript profiling of crown rootless1 mutant stem base reveals new elements
422 associated with crown root development in rice. *BMC Genom.* 12(1), 1-12.
423 <https://doi.org/10.1186/1471-2164-12-387>.
- 424 [dataset] Di Rienzo J.A., Casanoves F., Balzarini M.G., Gonzalez L., Tablada M.,
425 Robledo C.W. InfoStat versión 2018. Centro de Transferencia InfoStat, FCA,
426 Universidad Nacional de Córdoba, Argentina. URL <http://www.infostat.com.ar>.
- 427 [dataset] Di Rienzo, J.A., Guzmán, A.W., Casanoves, F., 2002. A multiple-
428 comparisons method based on the distribution of the root node distance of a binary
429 tree. *J. Agric. Biol. Environ. Stat.* 7(2), 129-142.
430 <http://doi.org/10.1198/10857110260141193>.
- 431 [dataset] Dong, C.F., Gu, H.R., Ding, C.L., Xu, N.X., Liu, N., Qu, H., Shen, Y.X.,
432 2012. Effects of gibberellic acid application after anthesis on the feeding value of
433 double-purpose rice (*Oryza sativa* L.) straw at harvest. *Field Crops Res.* 131, 75-80.
434 <https://doi.org/10.1016/j.fcr.2012.02.018>.

- 435 [dataset] Du, B., Wei, Z., Wang, Z., Wang, X., Peng, X., Du, B., Chen, R., Zhu, L.,
436 He, G., 2015. Phloem-exudate proteome analysis of response to insect brown plant-
437 hopper in rice. *J. Plant Physiol.* 183, 13-22.
438 <https://doi.org/10.1016/j.jplph.2015.03.020>.
- 439 [dataset] Dwiningsih, Y., Alkahtani, J., 2022. Phenotypic Variations, Environmental
440 Effects and Genetic Basis Analysis of Grain Elemental Concentrations in Rice (*Oryza*
441 *sativa* L.) for Improving Human Nutrition. Preprints 2022090263. [http://doi:](http://doi:10.20944/preprints202209.0263.v)
442 [10.20944/preprints202209.0263.v](https://doi.org/10.20944/preprints202209.0263.v).
- 443 [dataset] Fujita, M., Horiuchi, Y., Ueda, Y., Mizuta, Y., Kubo, T., Yano, K., Yamaki,
444 S., Tsuda, K., Nagata, T., Niihama, M., Kato, H., Kikuchi, S., Hamada, K., Mochizuki,
445 T., Ishimizu, T., Iwai, H., Tsutsumi, N., Kurata, N., 2010. Rice expression atlas in
446 reproductive development. *Plant Cell Physiol.* 51(12), 2060-2081.
447 <https://doi.org/10.1093/pcp/pcq165>.
- 448 [dataset] Garris, A.J., Tai, T.H., Coburn, J., Kresovich, S., McCouch, S., 2005.
449 Genetic structure and diversity in *Oryza sativa* L. *Genetics.* 169(3), 1631-1638.
450 <http://doi.org/10.1534/genetics.104.035642>.
- 451 [dataset] Gazquez, A., Maiale, S.J., Rachoski, M.M., Vidal, A., Ruiz, O., Menéndez,
452 A.B., Rodríguez, A.A., 2015. Physiological response of multiple contrasting rice
453 (*Oryza sativa* L) cultivars to suboptimal temperatures. *J. Agron. Crop Sci.* 201(2),
454 117-127. <http://doi.org/10.1111/jac.12095>.
- 455 [dataset] Gongora, S.Y., 2015. Development of Disease Resistant Rice Using Whole
456 Genome Sequencing and Standard Breeding Methods. Doctoral dissertation,
457 Louisiana State University, 3870.
458 https://digitalcommons.lsu.edu/gradschool_dissertations/3870
- 459 [dataset] Hill, W.G., 2001. Selective Breeding, in: Brenner, S., Miller, J.H. (Eds.),
460 *Encyclopedia of Genetics.* Academic Press, London, pp. 1796-1799.
- 461 Hörmann, F., Kuchler, M., Sveshnikov, D., Oppermann, U., Li, Y., Soll, J., 2004.
462 Tic32, an essential component in chloroplast biogenesis. *J. Biol. Chem.* 279(33),
463 34756-34762. <https://doi.org/10.1074/jbc.M402817200>.
- 464 [dataset] Kang, H.M., Sul, J.H., Service, S.K., Zaitlen, N.A., Kong, S.Y., Freimer,
465 N.B., Sabatti, C., Eskin, E., 2010. Variance component model to account for sample
466 structure in genome-wide association studies. *Nat. Genet.* 42(4), 348-354.
467 <https://doi.org/10.1038/ng.548>.

- 468 [dataset] Khan, M.H., Dar, Z.A., Dar, S.A., 2015. Breeding strategies for improving
469 rice yield—a review. *Agricultural Sciences*, 6(5), 467. 10.4236/as.2015.65046.
- 470 [dataset] Khan, N., Essemine, J., Hamdani, S., Qu, M., Lyu, M.J.A., Perveen, S.,
471 Stirbet., A., Govindjee Govindjee, Zhu, X.G., 2021. Natural variation in the fast phase
472 of chlorophyll a fluorescence induction curve (OJIP) in a global rice minicore panel.
473 *Photosynth. Res.* 150(1), 137-158. <https://doi.org/10.1007/s11120-020-00794-z>.
- 474 [dataset] Lakra, N., Kaur, C., Anwar, K., Singla-Pareek, S.L., Pareek, A., 2018.
475 Proteomics of contrasting rice genotypes: identification of potential targets for raising
476 crops for saline environment. *Plant Cell Environ.* 41(5), 947-969.
477 <https://doi.org/10.1111/pce.12946>.
- 478 [dataset] Liu, Y., Lin, Y., Gao, S., Li, Z., Ma, J., Deng, M., Chen, G., Wei, Y., Zheng,
479 Y., 2017. A genome-wide association study of 23 agronomic traits in Chinese wheat
480 landraces. *Plant J.* 91(5), 861-873. <https://doi.org/10.1111/tbj.13614>.
- 481 [dataset] McCouch, S.R., Wright, M.H., Tung, C.W., Maron, L.G., McNally, K.L.,
482 Fitzgerald, M., Singh, N., DeClerck, G., Agosto-Perez, F., Korniliev, P., Greenberg,
483 A.J., Naredo, M. E.B., Mercado, S.M.Q., Harrington, S.E., Shi, Y., Branchini, D.A.,
484 Kuser-Falcão, P. R., Leung, H., Eban, K., Yano, M., Eizenga, G., McClung, A.,
485 Mezey, J., 2016. Open access resources for genome-wide association mapping in
486 rice. *Nat. Commun.* 7(1), 1-14. <https://doi.org/10.1038/ncomms10532>.
- 487 [dataset] Puig, M.L., Rodríguez, A.A., Vidal, A.A., Bezus, R., Maiale, S.J., 2021.
488 Patterns of physiological parameters and nitrogen partitioning in flag leaf explain
489 differential grain protein content in rice. *Plant Physiol. Biochem.* 168, 457-464.
490 <https://doi.org/10.1016/j.plaphy.2021.10.034>
- 491 [dataset] Pyke, K.A., Leech, R.M., 1994. A genetic analysis of chloroplast division
492 and expansion in *Arabidopsis thaliana*. *Plant Physiol.* 104(1), 201-207.
493 <https://doi.org/10.1104/pp.104.1.201>.
- 494 [dataset] Raorane, M.L., Pabuayon, I.M., Varadarajan, A.R., Mutte, S.K., Kumar, A.,
495 Treumann, A., Kohli, A., 2015. Proteomic insights into the role of the large-effect QTL
496 qDTY 12.1 for rice yield under drought. *Mol. Breed.* 35(6), 1-14.
497 <https://doi.org/10.1007/s11032-015-0321-6>.
- 498 [dataset] Richards, R.A., Condon, A.G., Rebetzke, G.J., 2001. Traits to improve yield
499 in dry environments, in: Reynolds, M.P., Ortiz-Monasterio J.I., McNab, A. (Eds.),
500 *Application of Physiology in Wheat Breeding*. D.F.: CIMMYT, Mexico, pp. 88–100.

- 501 [dataset] Strasser, R.J., Srivastava, A., Tsimilli-Michael, M., 2000. The fluorescence
502 transient as a tool to characterize and screen photosynthetic samples, in: M. Yunus,
503 M, Pathre, U. (Eds.), Probing photosynthesis: Mechanisms, Regulation and
504 Adaptation. CRC Press, London, pp. 445-483.
- 505 [dataset] Takai, T., Fukuta, Y., Shiraiwa, T., Horie, T., 2005. Time-related mapping of
506 quantitative trait loci controlling grain-filling in rice (*Oryza sativa* L.). J. Exp. Bot.
507 56(418), 2107-2118. <https://doi.org/10.1093/jxb/eri209>.
- 508 [dataset] Tavakkoli, E., Fatehi, F., Rengasamy, P., McDonald, G.K., 2012. A
509 comparison of hydroponic and soil-based screening methods to identify salt
510 tolerance in the field in barley. J. Exp. Bot. 63(10), 3853-3867.
511 <http://doi.org/10.1093/jxb/ers085>
- 512 [dataset] Tobiasz-Salach, R., Kalaji, H.M., Mastalerczuk, G., Bąba, W., Bobrecka-
513 Jamro, D., Noras, K., 2019. Can photosynthetic performance of oat (*Avena sativa* L.)
514 plants be used as bioindicator for their proper growth conditions?. Chiang Mai J. Sci.
515 46, 880-895.
- 516 [dataset] Wada, Y., Miura, K., Watanabe, K., 1993. Effects of source-to-sink ratio on
517 carbohydrate production and senescence of rice flag leaves during the ripening
518 period. Jpn. J. Crop Sci. 62(4), 547-553. <https://doi.org/10.1626/jcs.62.547>.
- 519 [dataset] Weirich, A., Oliveira, B.H.N.D., Arend, E.B., Duarte, G.L., Ponte, L.R.,
520 Sperotto, R. A., Ricachenevsky, F.K., Fett, J.P., 2019. The combined strategy for iron
521 uptake is not exclusive to domesticated rice. Sci. Rep. 9(1), 1-17.
522 <https://doi.org/10.1038/s41598-019-52502-0>.
- 523 [dataset] Wang, Y., Zhang, J., Yu, J., Jiang, X., Sun, L., Wu, M., Chen, G., Lv, C.,
524 2014. Photosynthetic changes of flag leaves during senescence stage in super high-
525 yield hybrid rice LYPJ grown in field condition. Plant Physiol. Biochem. 82, 194-201.
526 <https://doi.org/10.1016/j.plaphy.2014.06.005>
- 527 [dataset] Wang, Y., Zhang, Y., Zhang, Q., Cui, Y., Xiang, J., Chen, H., Wang, X.,
528 Zhu, D., Zhang, Y., 2019. Comparative transcriptome analysis of panicle
529 development under heat stress in two rice (*Oryza sativa* L.) cultivars differing in heat
530 tolerance. PeerJ. 7, e7595. <https://doi.org/10.7717/peerj.7595>.
- 531 [dataset] Wang, Z.Q., Xu, X.Y., Gong, Q.Q., Xie, C., Fan, W., Yang, J.L., Lin, Q.S.,
532 Zheng, S.J., 2014. Root proteome of rice studied by iTRAQ provides integrated
533 insight into aluminum stress tolerance mechanisms in plants. J. Proteom. 98, 189-
534 205. <https://doi.org/10.1016/j.jprot.2013.12.023>.

535 [dataset] Xing, Y., Zhang, Q., 2010. Genetic and molecular bases of rice yield. Annu.
536 Rev. Plant Biol. 61, 421-442. [https://doi.org/10.1146/annurev-arplant-042809-](https://doi.org/10.1146/annurev-arplant-042809-112209)
537 112209.

538 [dataset] Zhang, H., Yu, Z., Yao, X., Chen, J., Chen, X., Zhou, H., Lou, Y., Ming, F.,
539 Jin, Y., 2021. Genome-wide identification and characterization of small auxin-up RNA
540 (SAUR) gene family in plants: evolution and expression profiles during normal growth
541 and stress response. BMC Plant Biol. 21(1), 1-14. [https://doi.org/10.1186/s12870-](https://doi.org/10.1186/s12870-020-02781-x)
542 020-02781-x.

543 [dataset] Zhang, M., Shan, Y., Kochian, L., Strasser, R.J., Chen, G., 2015.
544 Photochemical properties in flag leaves of a super-high-yielding hybrid rice and a
545 traditional hybrid rice (*Oryza sativa* L.) probed by chlorophyll a fluorescence
546 transient. Photosynth. Res. 126(2), 275-284. [https://doi.org/10.1007/s11120-015-](https://doi.org/10.1007/s11120-015-0151-8)
547 0151-8.

548 [dataset] Zhao, K., Tung, C.W., Eizenga, G.C., Wright, M.H., Ali, M.L., Price, A.H.,
549 Norton G. J., Islam M.R., Reynolds, A., Mezey J., McClung, A.M., Bustamante, C.D.,
550 McCouch, S.R., 2011. Genome-wide association mapping reveals a rich genetic
551 architecture of complex traits in *Oryza sativa*. Nat. Commun. 2(1), 1-10.
552 <http://doi.org/10.1038/ncomms1467>.

553 [dataset] Zhao, Q., Liu, C., 2017. Chloroplast chaperonin: an intricate protein folding
554 machine for photosynthesis. Front. Mol. Biosci. 4, 98.
555 <https://doi.org/10.3389/fmolb.2017.00098>.

556 [dataset] Zhao, Y., Christensen, S.K., Fankhauser, C., Cashman, J.R., Cohen, J.D.,
557 Weigel, D., Chory, J., 2001. A role for flavin monooxygenase-like enzymes in auxin
558 biosynthesis. Science. 291(5502), 306-309.
559 <https://doi.org/10.1126/science.291.5502.306>.

560 [dataset] Živčák, M., Brestič, M., Olšovská, K., Slamka, P., 2008. Performance index
561 as a sensitive indicator of water stress in *Triticum aestivum* L. Plant Soil Environ.
562 54(4), 133-139.

563

564

565 **Figure legends**

566

567 **FIGURE 1.** PCA of yield and OJIP parameters data from genotypes with contrasting
568 in grain yield at anthesis stage. HY, genotypes with high yield; NY, genotypes with
569 normal yield. Yield parameters: Grains $\cdot m^{-2}$, number of grains per m^{-2} ; Y, Kg of
570 grains $\cdot ha^{-1}$. OJIP parameters: F_V/F_M , maximum photochemical efficiency of PSII;
571 ΨE_0 , maximum efficiency of electron transport in PSII beyond reduced quinone A;
572 γRC , density of active PSII reaction centre; PI_{ABS} , performance index.

573

574 **FIGURE 2.** Linear regression analysis of PI_{ABS} and Y data from genotypes with
575 contrasting in grain yield at the anthesis stage. The model's goodness of fit was
576 determined by the coefficient of determination R square (r^2). The solid line in each
577 graph represents the best regression linear fit model between dependent (Y-axis)
578 and independent (X-axis) variables.

579

580 **FIGURE 3.** GWAS using PI_{ABS} determined in plants of the rice diversity panel RDP1
581 at tillering stage. **A.** Manhattan plot using the RDP1 genotyping and the PI_{ABS}
582 phenotyping. The x-axis shows the SNPs along each chromosome; the y-axis is the
583 $-\log_{10}(p\text{-value})$ for the association. Gray and white circles above dotted line represent
584 significant SNPs with $-\log_{10}(p\text{-value}) > 4$. The gray circles correspond to SNPs
585 registered in GWAS with PI_{ABS} phenotyping. The white circles correspond to
586 significant SNPs registered in GWAS with PI_{ABS} phenotyping but also with ΨE_0 and
587 γRC phenotyping. **B.** Pie chart with results of gene percentages for each subcellular
588 location obtained by a protein subcellular localization prediction analysis. **C.** QTL
589 region in the GWAS peak on chromosome 9 enrichment with chloroplastic genes.
590 The horizontal bar shows a physical map of chromosome 9 (21.6–22.9 Mb); the
591 chloroplastic genes with associated or uncharacterized functions were represented
592 by unfilled or filled arrows, respectively. **D.** The main haplotypes associated to from
593 candidate chloroplastic genes with contrasting haplotypes for PI_{ABS} were analyzed.
594 Grey and white bars represent haplotypes associated with PI_{ABS} average high and
595 low values, respectively (ANOVA and post hoc analysis DGC tests $p < 0.05$, $n = 5$
596 per genotype; Different letters represent significant differences between haplotypes).

597

598 **FIGURE 4.** PCAs of PI_{ABS} average value per haplotype and PI_{ABS} per genotype data.
599 HP and LP haplotypes associated with each $CGPI_{ABS}$. **A.** the dots represent CP1 and

600 CP2 values associated with HP and LP haplotypes. **B.** the dots represent CP1 and
601 CP2 values associated with genotypes from each *O. sativa* subpopulation.

602

603 **FIGURE 5.** Panicle weight distribution within the *O. sativa* structure population. PW
604 was determined in plants of the rice diversity panel RDP1 at the end of the filling
605 grain. Gray (*Japonica* spp. genotypes) and white (*Indica* spp. genotypes) represent
606 means \pm S.E. Different letters represent significant differences between
607 subpopulations (ANOVA and post hoc analysis DGC tests, $p < 0.05$, $n = 3$ per
608 genotype). Asterisks represent significant differences between subspecies (Student's
609 t-test, two samples; **** $p < 0.0001$; $n = 3$ per genotype).

610

611

612

613

614

615

616

617

618

619

620

621

622

623

624

625

626

627

628

629

630

631

632

633

634 **Figure 1**

635

636

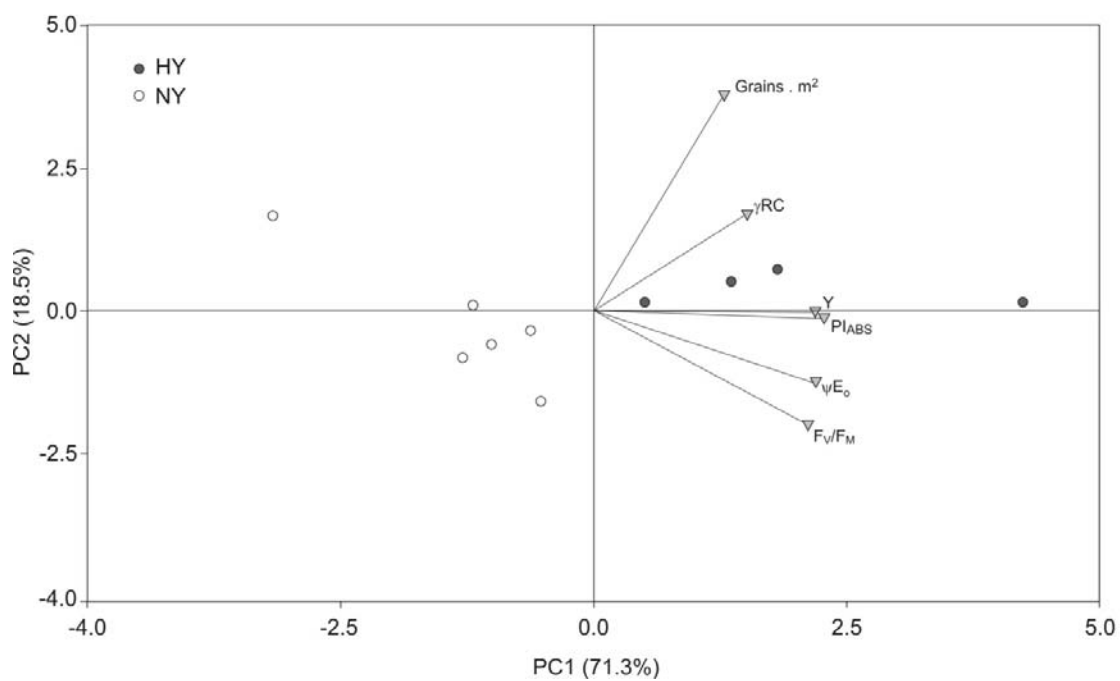
637

638

639

640

641



642

643

644

645

646

647

648

649

650

651

652

653

654 **Figure 2**

655

656

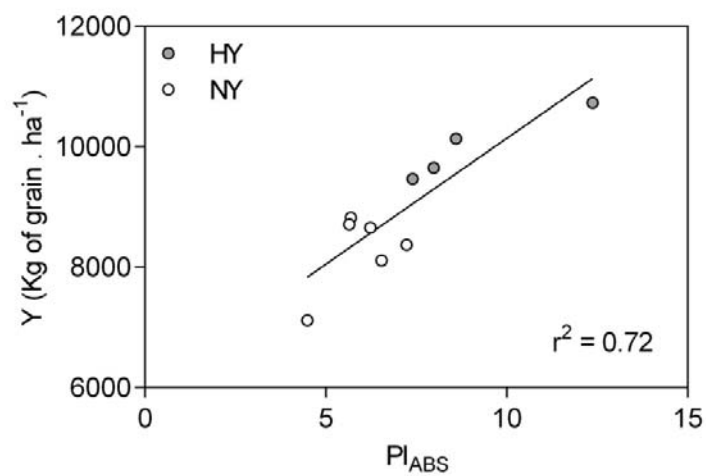
657

658

659

660

661



662

663

664

665

666

667

668

669

670

671

672

673

674

675

676

677

678 **Figure 3**

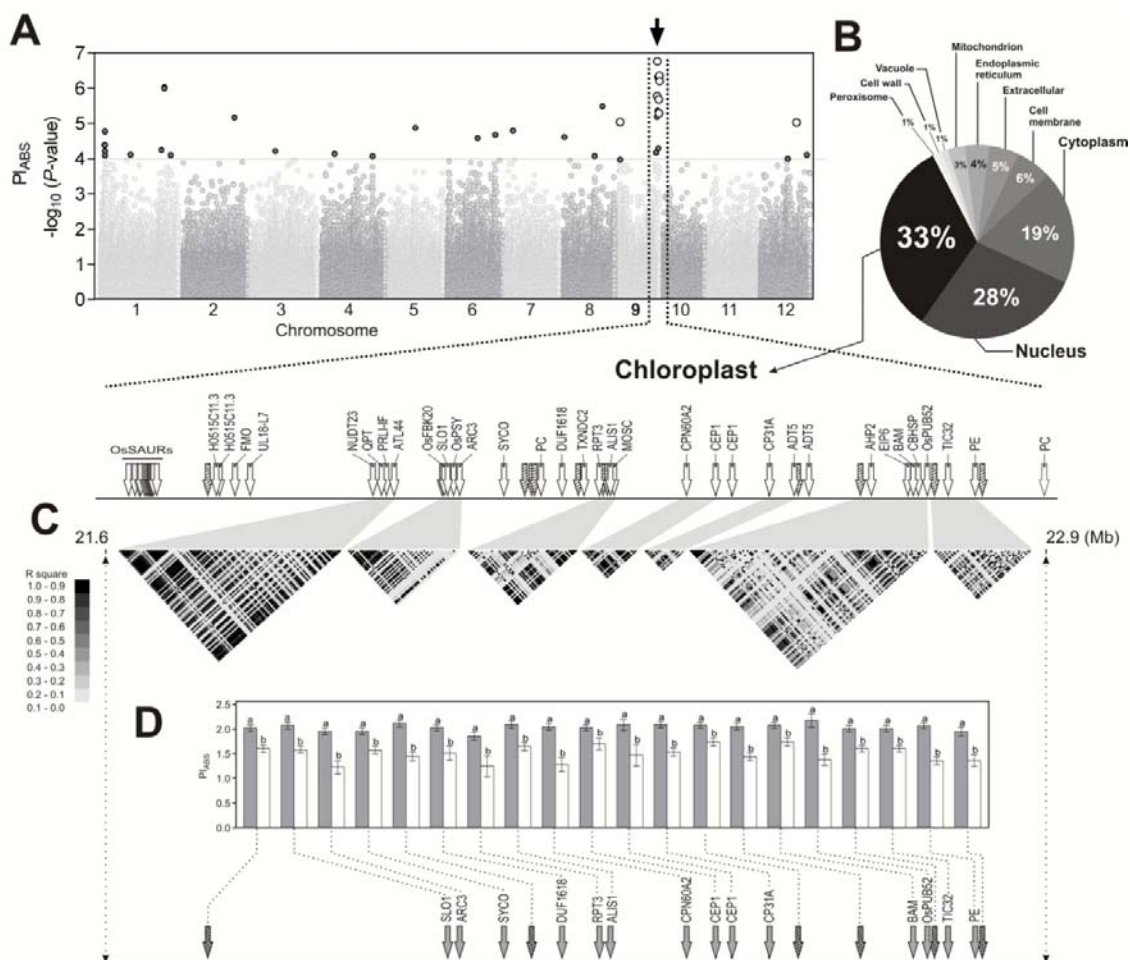
679

680

681

682

683



684

685

686

687

688

689

690

691

692

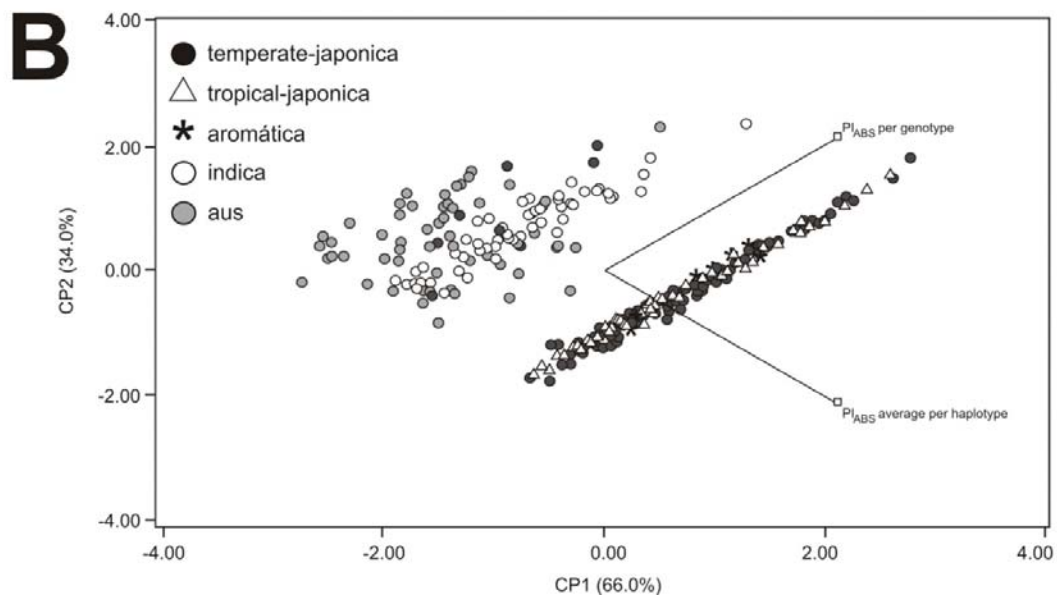
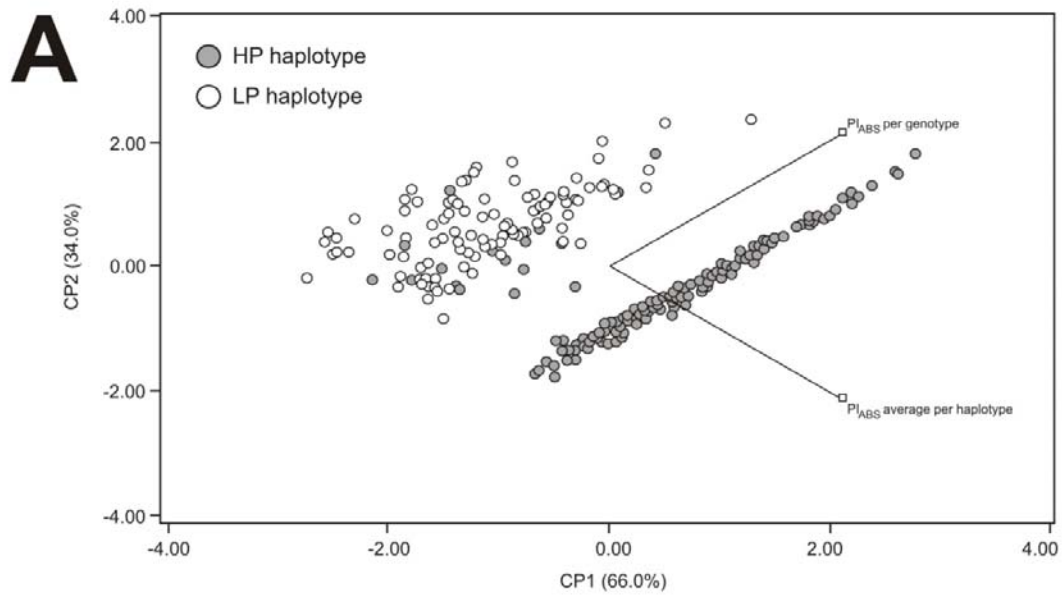
693 **Figure 4**

694

695

696

697



698

699

700

701 **Figure 5**

702

703

704

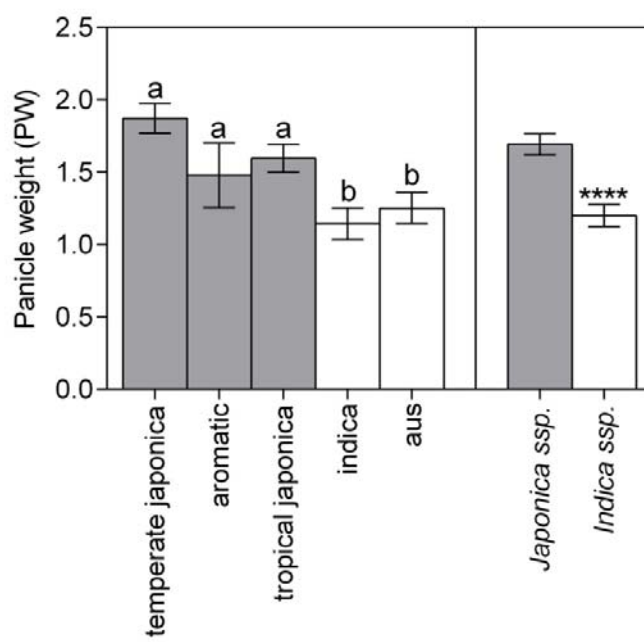
705

706

707

708

709



710

Table 1. Correlation matrix of structure and functional parameters of the photosynthetic apparatus in rice flag leaf with yield parameters. The matrix correlation presents the Pearson r values and its corresponding P values to each correlation between the different parameters.

	Kg . m ⁻²	grains . m ⁻²	PI _{ABS}	ψE _O	F _V /F _M	γRC
Kg . m ⁻²	1	0.0266	0.0039	0.0034	0.0169	0.0212
grains . m ⁻²	0.73	1	0.1711	0.0834	0.2262	0.4209
PI _{ABS}	0.85	0.50	1	<0.0001	<0.0001	0.0007
ψE _O	0.85	0.61	0.97	1	0.0002	0.0120
F _V /F _M	0.76	0.45	0.97	0.94	1	0.0022
γRC	0.75	0.31	0.91	0.79	0.87	1

Table 2. Description of genes from the GWAS peak on chromosome 9 of proteins with chloroplastic subcellular localization

gene ID	Gene Symbol	Description
LOC_Os09g37350	OsSAUR40	Small auxin-UPA 40 Auxin responsive SAUR protein family protein
LOC_Os09g37369	OsSAUR41	Small auxin-UP RNA 41 Auxin responsive SAUR protein family protein
LOC_Os09g37394	OsSAUR44	Small auxin-UP RNA 44 Auxin responsive SAUR protein family protein
LOC_Os09g37400	OsSAUR45	Small auxin-UP RNA 45 Auxin responsive SAUR protein family protein
LOC_Os09g37420	OsSAUR47	Small auxin-UP RNA 47 Auxin responsive SAUR protein family protein
LOC_Os09g37430	OsSAUR48	Small auxin-UP RNA 48 Auxin responsive SAUR protein family protein
LOC_Os09g37440	OsSAUR49	Small auxin-UP RNA 49 Auxin responsive SAUR protein family protein
LOC_Os09g37452	OsSAUR50	Small auxin-UP RNA 50 Auxin responsive SAUR protein family protein
LOC_Os09g37460	OsSAUR51	Small auxin-UP RNA 51 Auxin responsive

		SAUR protein family protein
		Small auxin-UP RNA
		52 Auxin responsive
LOC_Os09g37470	OsSAUR52	SAUR protein family protein
		Small auxin-UP RNA
		53 Auxin responsive
LOC_Os09g37480	OsSAUR53	SAUR protein family protein
		Small auxin-UP RNA
		54 Auxin responsive
LOC_Os09g37490	OsSAUR54	SAUR protein family protein
		Small auxin-UP RNA
		55 Auxin responsive
LOC_Os09g37500	OsSAUR55	SAUR protein family protein
LOC_Os09g37610		Uncharacterized protein
		FAD dependent oxidoreductase family protein
LOC_Os09g37650	H0515C11.3	Flavin-containing monooxygenase FMO family protein
LOC_Os09g37690	FMO	Ribosomal protein L18P/L5E family protein
LOC_Os09g37740	UL18-L7	NUDIX hydrolase domain containing protein
LOC_Os09g38040	NUDT23	
LOC_Os09g38060	QPT	NADC homolog
LOC_Os09g38070	PRLI-interacting factor	PRLI-interacting factor A
LOC_Os09g38110	ATL44	Probable E3 ubiquitin-protein ligase ATL44

LOC_Os09g38268		Uncharacterized protein
LOC_Os09g38300		Uncharacterized protein Protein prenyltransferase domain containing
LOC_Os09g38310	SLO1	protein Chloroplast phytoene synthase 3
LOC_Os09g38320	OsPSY	MORN motif repeat containing protein
LOC_Os09g38330	ARC3	CysteinyI-tRNA synthetase, class Ia family protein
LOC_Os09g38420	SYCO	Uncharacterized protein
LOC_Os09g38490		Uncharacterized protein
LOC_Os09g38510		Uncharacterized protein
LOC_Os09g38520		Uncharacterized protein plastocyanin-like domain containing
LOC_Os09g38540	PC	protein, putative, expressed Domain of unknown function DUF1618
LOC_Os09g38600	DUF1618	domain containing protein
LOC_Os09g38650		Uncharacterized protein
LOC_Os09g38670		Thioredoxin domain 2 containing protein
LOC_Os09g38720	RPT3	Regulatory particle triple-A ATPase 3
LOC_Os09g38740		Uncharacterized protein

LOC_Os09g38750		Uncharacterized protein
LOC_Os09g38759	ALIS1	Protein of unknown function DUF284 Molybdenum cofactor sulfurase, C-terminal domain containing
LOC_Os09g38772	MOSC	protein GroEL-like chaperone,
LOC_Os09g38980	CPN60A2	ATPase
LOC_Os09g39070	CEP1	Peptidase C1A, papain family protein
LOC_Os09g39110	CEP1	Peptidase C1A, papain family protein
LOC_Os09g39180	CP31A	Similar to Nucleic acid-binding protein precursor
LOC_Os09g39230	ADT5	Prephenate dehydratase domain containing protein
LOC_Os09g39240		Uncharacterized protein
LOC_Os09g39260	ADT5	Prephenate dehydratase domain containing protein
LOC_Os09g39360		Uncharacterized protein
LOC_Os09g39400	AHP2	Histidine-containing phosphotransfer 2 protein
LOC_Os09g39560	EIP6	Haloacid dehalogenase-like hydrolase domain containing protein
LOC_Os09g39570	BAM	Beta-amylase (1,4-alpha-D-glucan maltohydrolase)

LOC_Os09g39580		Similar to Calmodulin-binding heat-shock protein
LOC_Os09g39620	OsPUB52	Serine/threonine protein kinase-related domain containing protein
LOC_Os09g39630		Uncharacterized protein
LOC_Os09g39670	TIC32	Similar to Short-chain dehydrogenase Tic32
LOC_Os09g39760	PE	Pectinesterase
LOC_Os09g39790		Uncharacterized protein
LOC_Os09g39940	PC	plastocyanin-like domain containing protein, putative, expressed
